**Melatonin behavior in restoring chemical damaged C2C12 myoblasts**

Sara Salucci*, Valentina Baldassarri*, Barbara Canonico, Sabrina. Burattini, Michela Battistelli, Michele Guescini, Stefano Papa, Vilberto Stocchi, Elisabetta Falcieri

Department of Biomolecular Sciences, University of Urbino Carlo Bo. Via Saffi 2, 61029, Urbino, Italy.

Corresponding author: **Dr. Sara Salucci**

Department of Earth, Life and Environmental Sciences, University of Urbino "Carlo Bo". Via Ca' le Suore 2, 61029, Urbino, Italy.

E-mail: sara.salucci@uniurb.it

Author's e-mail addresses:

valentina.baldassarri@uniurb.it

sara.salucci@uniurb.it

barbara.canonico@uniurb.it

sabrina.burattini@uniurb.it

michela.battistelli@uniurb.it

michele.guescini@uniurb.it

stefano.papa@uniurb.it

vilberto.stocchi@uniurb.it

elisabetta.falcieri@uniurb.it

*Dr. Dr. V. Baldassarri and S. Salucci contributed equally to this work.

Authors declare no conflict of interest, having no commercial relationships to products or companies related to the subject matter of the article.

All authors gave substantial contributions to the conception and design of the work and to the acquisition, analysis, and interpretation of data.

**ABSTRACT**

It is known that, besides a wide range of functions, melatonin provides protection against oxidative stress, thanks to its ability to act, directly, as a free radical scavenger and, indirectly, by stimulating anti-oxidant enzyme production and mitochondrial electron transport chain efficiency.

Oxidative stress is one of the major players in initiating apoptotic cell death in skeletal muscle, as well as in other tissues. Apoptosis is essential for skeletal muscle development and homeostasis; nevertheless, its misregulation has been frequently observed in several myopathies, in sarcopenia, as well as in denervation and disuse.

Melatonin activity was investigated in undifferentiated C2C12 skeletal muscle cells, after exposure to various apoptotic chemical triggers, chosen for their different mechanisms of action. Cells were pre-treated with melatonin and then exposed to hydrogen peroxide, etoposide and staurosporine. Morpho-functional and molecular analyses show that in myoblasts melatonin prevents oxidative stress and apoptosis induced by chemicals following, at least in part, the mitochondria pathway.

These results confirm melatonin ability to act as an anti-oxidant and anti-apoptotic molecule in muscle tissue, thus suggesting a possible therapeutic strategy for myopathies involving apoptosis misregulation.

**KEYWORDS:** melatonin, skeletal muscle apoptosis, oxidative stress, mitochondria

**INTRODUCTION**

Apoptosis is fundamental for skeletal muscle physiology since it plays a key role in coordinating myoblast proliferation and muscle differentiation (Shiokawa et al., 2002; Battistelli et al., 2014). In addition, it is involved in several pathological conditions, such as sarcopenia and disuse muscle atrophy (Marzetti et al., 2010; Teixeira et al., 2012), myotonic dystrophy (Loro et al, 2010), Duchenne muscular dystrophy (Abdel-Salam et al., 2009; Davis et al., 2013), collagen myopathies (Merlini et al., 2008) and others.

Melatonin (MEL), or N-acetyl-5-methoxytryptamine, has been identified as a remarkable molecule with various physiologic actions promoting protection in many cell types (Teodoro et al., 2014). Numerous studies have demonstrated that MEL has anti-apoptotic effects in normal cells (Jou et al., 2004; Yoo and Jeung, 2009; Han et al., 2011; Salucci et al., 2014a) which can be attributed to its antioxidant properties (Paradies et al., 2010; Galano et al., 2011). In fact, it counteracts a variety of reactive oxygen species (ROS) acting as a direct radical scavenger (Hardeland et al., 2009; Salucci et al., 2014b). It also has an indirect activity, by stimulating the production of anti-oxidant enzymes (e.g. glutathione peroxidase, glutathione reductase, γ-glutamylcysteine synthetase) and by increasing electron transport chain efficiency at the level of mitochondrial cristae (Ding et al., 2014; Zhang and Zhang, 2014).

Thanks to its structure that is both water-soluble and fat-soluble, MEL is able to diffuse through all the biological membranes, also overcoming the blood-brain barrier and the placenta. Due to this property, it is present in moderate amounts in the cell nucleus, where it protects DNA from oxidative damage (Reiter et al., 2007).

Excessive ROS levels are key initiators and mediators of dysfunctions in a variety of cells including muscle cells. ROS mediated disruptions in cell signaling, metabolism, transcriptional activity, mitochondrial function, and increased apoptotic pathway activation (Marzetti et al., 2013; SullivanGunn and Lewandowski, 2013). Atrophy and some myopathies are

associated with excessive ROS levels, which increase mitochondrial damage, and in turn, contribute to mitochondrially mediated apoptotic signaling (Bennett et al., 2013; Vasilaki and Jackson, 2013; Derbrè et al., 2014; Barbieri et al., 2015). If molecules with antioxidant capacities can counteract the oxidative damage, they may also play a key role in preventing the onset of oxidative stress conditions leading to cell death. In literature we can find numerous evidences which indicate that MEL leads to an improvement of certain muscle pathological conditions thanks to its ability to normalize or prevent oxidative stress (Chen et al., 2009; Hibaoui et al., 2009; Chahbouni et al., 2010; Stratos et al., 2012).

So, given the previous researches and the known anti-oxidant properties of MEL, the aim of our work was to test by means of morpho-functional and molecular analyses MEL effects on the cytotoxicity induced by various chemical triggers, in C2C12 myoblasts, thereby verifying its ability to prevent oxidative stress and apoptosis.

## MATERIALS AND METHODS

### Cell culture and treatments

C2C12 adherent myoblasts were grown as previously described (Salucci et al., 2013).

Cells were monitored using a Nikon Eclipse TE 2000-S inverted microscope (IM) equipped with a DN 100 Nikon digital camera system.

The best treatments for apoptosis induction, discussed and established in an our previous work (Salucci et al., 2010a, 2013), were:

- 25 µm etoposide, for 24 hours
- 0.25 µm staurosporine, for 5 hours
- 500 µm hydrogen peroxide ($H_2O_2$), for 5 hours

Different MEL doses (1mM, 500µM 100µM and 50µM) have been employed to evaluate the better hormone concentration which does not affect cell viability and proliferation. On the basis of our experimental results and of literature data (Hibaoui et al, 2009), 100µM MEL appears the best treatment. Thus, samples were pre-incubated with 100 µM MEL, 24 hours before apoptosis induction.

For each technique, control sample and 24 hour- MEL treatment were also analyzed. MEL(Sigma, St Louis, MO, USA) was first dissolved in absolute ethanol at the initial concentration of 100 mM, and then diluted at the final 100 µM concentration in culture medium.

To ensure cellular viability the trypan blue (TB) exclusion assay was carried out. It has been established that cell membrane integrity is a basic criterion for distinguishing dead from live cells. The TB method is a very common assay for evaluating cytotoxicity in experimental investigations where dead cells absorb TB into the cytoplasm because of membrane integrity loss, whereas live cells remain unstained (Avelar-Freitas et al., 2014). Thus, the relative number of dead and live cells is obtained by optical microscopy by counting the number of stained (dead) and unstained (live) cells using the Neubauer chamber.

### Scanning electron microscopy (SEM)

Cells, directly processed on coverslips in Petri dishes, were fixed *in situ* with 2.5% glutaraldehyde for 40 minutes and post-fixed in 1% Osmium tetroxide ($OsO_4$) for 1 hour. Samples were dehydrated using increasing ethanol concentrations, then they were dried in a 1:1 mixture of absolute ethanol and hexamethyldisilazane (HMDS) and then with pure HMDS. Finally, slides were mounted on aluminum stubs and sputter-coated with gold. Samples were observed using a Philips 515 scanning electron microscope (Salucci et al., 2010b, 2013).

**Transmission electron microscopy (TEM)**

Cells, grown in flasks, were rinsed in 0.15 M phosphate buffer (pH 7.4), were fixed *in situ* with 2.5% glutaraldehyde for 40 minutes, and then they were gently scraped, centrifuged and post-fixed in 1% $OsO_4$ for 1 hour. Pellets were dehydrated, using increasing concentrations of ethanol, and embedded in araldite.

Ultrathin sections were stained with uranyl acetate and lead citrate and then analyzed using a Philips CM10 electron microscope (Battistelli et al., 2011; Burattini et al., 2013).

**Confocal laser scanning microscopy (CLSM)**

For CLSM analysis, immunofluorescence (IF) techniques were carried out on coverslips. Samples were rinsed with 0.1 M PBS pH 7.4 and fixed *in situ* with 4% paraformaldehyde in PBS, for 30 minutes at room temperature (R.T.).

For the TUNEL technique, after a further washing with PBS, samples were permeabilized with a 2:1 mixture of ethanol and acetic acid, for 5 minutes at -20°C. Procedures were carried out according to the manufacturer's instructions and all reagents were part of the Apoptag Plus kit (D.B.A.). Briefly, cells were treated with the terminal deoxynucleotidyl transferase (TdT) buffer for 10 minutes at R.T. and incubated with the reaction buffer containing the TdT enzyme for 1 hour, at 37°C in a humidified chamber (Salucci et al., 2014a). The reaction was blocked using the stop buffer for 10 minutes. Cells were incubated with a FITC-conjugated anti-digoxigenin antibody for 30 minutes at R.T.

For mitochondrial analysis, 50 nM NAO for 10 minutes was used. NAO fluorescence intensity has been quantified using Image J Software, on an established cell number (1 hundred cells ) for each condition.

Slides were finally mounted with an anti-fading medium (Vectashield, Vector Labs). Images were collected with a Leica TCS-SP5 Confocal connected to a DMI 6000 CS Inverted Microscope (Leica Microsystems CMS GmbH) and analyzed using the Leica Application Suite Advanced Fluorescence (LAS AF) software. Samples were examined using oil immersion objective lenses (40x N.A. 1.25; 63x N.A. 1.40). Excitation was at 488 nm (FITC and NAO); emission signals were detected at 519 nm (NAO) or 525 nm (FITC). CLSM images are presented as single-plane images or Z-stack projections.

**Flow cytometry (FC)**

Samples were acquired as fresh cells for MitoSOX, CM-H2DCFDA and NAO tests. To label fresh cells, we added each fluorochrome in the appropriate volume to cell suspension.

MitoSOX Red is a dye specifically targeted to mitochondria in live cells, it is readily oxidized by superoxide but not by other sources of reactive oxygen or nitrogen species and it produces red fluorescence. MitoSOX is hexyl triphenylphosphonium conjugated to hydroethidine (HE); while both HE and MitoSOX can be oxidized by mitochondrial superoxide, only the later can be used to detect mitochondrial specific oxidation when excited at selective wavelength (Robinson et al., 2006).

Detached myoblasts were loaded with MitoSOX Red 2 mM, maintained at R.T. for 20 min, until the cytometric analyses.

The fluorescent probe CM-H2DCFDA is a chloromethyl derivative of 2',7'-dichlorodihydrofluorescein diacetate ($H_2$DCFDA), useful as an indicator for ROS in cells, in particular for $H_2O_2$ detection. CM-H2DCFDA (Molecular Probes, OR) was added, for 30 min. at 37°C, to PBS of cellular pellets at the 10μM final concentration. Then cells were washed once with PBS.

The cardiolipin-sensitive probe 10-nonyl acridine orange (NAO) was used to monitor mitochondrial lipid changes (Canonico et al., 2014); cells were incubated with 100 nM NAO, for 20 minutes at 37°C.

At least 10.000 events were acquired for each sample, by means of a FACScalibur flow cytometer equipped with two lasers (Canonico et al., 2014). Data were acquired and analyzed using Cell TM Quest flow cytometry software (Becton Dickinson, San Jose, CA)

**Western blotting analysis**

Western blot analysis was performed as reported in Guescini et al., 2010. Briefly, samples containing 30 µg of protein were mixed with Laemmli sample buffer (1:1 ratio) and loaded onto 12% SDS-PAGE gels. Subsequently, proteins were blotted to a nitrocellulose membrane (GE Healthcare), primary antibodies used was Caspase-3 (1:1000 dilution, clone 8G10 Cell Signaling). Primary antibodies were incubated overnight at 4°C, followed by washing and the application of secondary HRP-conjugated antibody (Millipore). Immune complexes were visualized using the Supersignal Dura reagent (BioFix). Quantification was achieved using Quantity ONE software (BIORAD).

**Statistical analyses**

All data are presented as mean ± standard deviation of the mean. Student's t-test was applied for statistical analyses to compare results. p=.05 was considered as significance threshold.

**RESULTS**

**TB, ultrastructural and CLSM analyses**

To quantify and evaluate trigger ability in inducing cell death and MEL action against chemicals, a viability test at IM has been used. The TB exclusion assay allowed us to perform a cell count (in triplicate for all experimental conditions) and to construct histogram where (Fig. 1) dead cell fraction includes both apoptotic and necrotic cells.

Different MEL concentrations have been evaluated (1mM, 500µM, 100µM, 50µM) evidencing that, at higher doses, the dead cell fraction is not negligible. On the other hand, at lower doses (i.e. 100µM, 50µM) dead cell fraction is comparable to that observed in control condition (fig.1A), demonstrating that the hormone does not affect cell viability and proliferation. 100µM MEL is the concentration chosen to potentially prevent cell death induction, as suggested by literature data (Hibaoui et al, 2009), and by evaluating its action against $H_2O_2$. The latter data demonstrate that a 100µM MEL dose compared to 50 µM one significantly prevents cell damage (Fig. 1B).

Graph 1C reveals that all chemicals cause cell death, even if in different percentages, and that MEL reduces the fraction of dead cells. As evidenced by the Student's t-test, in the case of $H_2O_2$ treatment this reduction appears to be highly statistically significant ($p < 0.01$); in the case of etoposide the reduction is significant too, but to a lesser extent ($p < 0.05$). With staurosporine there is no statistical significance although a small decrease is observable.

This data has been confirmed after ultrastructural observations. Control myoblasts appeared fusiform or star-shaped, tightly adherent to the substrate (Fig. 2A), with preserved cytoplasmic organelles and nuclear components (Fig. 2B). The TUNEL technique does not reveal any nuclear labeling (Fig. 2C) and NAO fluorescence appears very intense, demonstrating a good mitochondrial condition (Fig. 2D). Myoblasts treated with 100 µM MEL do not reveal any changes compared to the control condition (Fig. 2E,F), showing that the hormone dose does not affect neither the nuclear behavior (Fig. 2G) nor the mitochondria activity (Fig. 2H).

$H_2O_2$ treatment causes cell rounding, detachment of many myoblasts and bleb formation (Fig. 3A); in the cytoplasm altered mitochondria and autophagic or aqueous vacuoles are visible (Fig. 3B), secondary necrosis with chromatin condensation also appears (Fig. 3C). TUNEL reaction is clearly positive (Fig. 3D) while NAO staining appears weak, indicating

cardiolipin oxidation (Fig. 3E). MEL pre-treatment protects myoblasts from $H_2O_2$. In fact, cells appear similar to the control condition (Fig. 3F-I).

Most myoblasts treated with etoposide appear fusiform, albeit in the presence of ultrastructural changes; membrane blebbing is evident and some apoptotic bodies can be seen (Fig. 4A). Intriguingly, in some cells this chemical induces the formation of condensed micronuclei and seems to better reflect the characteristics of 'classic' apoptosis (Fig. 4B). Etoposide induces in situ nuclear fragmentation (Fig. 4C); NAO fluorescence is weaker compared to the control sample, and also in Fig. 4D micronuclei can be observed (arrows). MEL pre-treatment prevents cell damage induced by etoposide: myoblast surface appears relatively smooth (Fig. 4E) and they show well-preserved organelles, complex autophagic vacuoles and non-apoptotic nuclei (Fig. 4F). The nuclear staining results almost negative, although some TUNEL-positive detached myoblasts are present (Fig. 4G). A bright NAO fluorescence is also visible (Fig. 4H).

After just 5 hours of staurosporine exposure a powerful effect can be observed on myoblasts. Cytoplasm shrinkage is evident and myoblasts assume a "spider-like" shape, with the formation of thin cytoplasm protrusions and the presence of small membrane blebs (Fig. 5A); numerous apoptotic bodies, containing condensed chromatin, are visible and cells in secondary necrosis also appear (Fig. 5B). At CLSM, cell morphology appears clearly compromised, TUNEL is strongly positive (Fig. 5C) and NAO labeling results uniform and quite weak (Fig. 5D). Although to a lesser extent compared to the other experimental conditions, MEL pre-treatment seems to protect staurosporine-treated cells from apoptosis. Some myoblasts retain their shape the others appear rounded (Fig. 5E). Within the nuclei euchromatin and nucleoli are visible, in the presence of a relatively good cytoplasmic preservation (Fig. 5F). At CLSM, we observe that MEL pre-treatment only partially induces a TUNEL positivity decrease but, as already observed at SEM and TEM, it certainly causes an improvement of the cell morphology (Fig. 5G). Even the mitochondrial activity seems to be improved (Fig. 5H).

NAO mean fluorescence in control and in treated samples for each experimental condition, has been quantified and an histogram (Fig.6) has been carried out in order to evaluate the differences between the trigger treatment alone and those pre-incubated with MEL. All triggers are able to induce a mitochondria fluorescence decrease, due to cardiolipin oxidation. MEL administration before cell death induction, maintained a mitochondria fluorescence comparable to control condition, evidencing an important MEL role in preventing cardiolipin oxidation and as a consequence mitochondria membrane integrity loss. This result is statistically significant in the case of $H_2O_2$ ($p<0.01$, **) and etoposide ($p<0.05$, *). MEL has no a significant protective effect against staurosporine treatment suggesting that staurosporine mechanism of action involved as secondary choice the mitochondrial pathway.

**FC and Western Blotting analyses**

Mitochondria play a fundamental role in apoptosis and, through mitochondrial membrane permeabilization and release of proapoptotic factors from the mitochondrial intermembrane space to the cytosol, they can be triggered by increased reactive oxygen and nitrogen species. Therefore, we studied the changes in mitochondrial superoxide generation and ROS production (Fig. 7A).

The formation of mitochondrial ROS (mtROS) is dependent on $\Delta\Psi_m$ (Korsehunov et al, 1997), and mtROS level increases exponentially as $\Delta\Psi_m$ is hyperpolarized (Lee et al., 2002; Storz et al., 2007). In myoblasts, our data illustrates different protection rates on ROS levels by MEL, depending on different triggers, moreover this rescue seems to be modulated on specific radical oxygen species.

$H_2O_2$ stimulates both superoxide anion and hydrogen peroxide formation, intriguingly MEL decreases $O_2^{\cdot -}$ levels of about 40%, whereas it blocks $H_2O_2$ formation only for a moderate extent (15%). Etoposide stimulates large amounts of intracellular hydrogen peroxide (at the considered time points) and MEL significantly decreases this ROS of about 17%. Finally, staurosporine didn't induce relevant $O_2^{\cdot -}$ amount (mitoSOX data) and consequently MEL didn't seem to act on this radical species but, weakly (5-6%), on $H_2O_2$ levels. These data contribute to the composed scenario of the multiple scavenging effects of MEL.

In addition, the appearance of cells with low NAO fluorescence intensity (NAO dim events) indicates mitochondria degeneration of structural cardiolipin. In fact, cardiolipin is subjected to peroxide oxidation by cytochrome *c* in the presence of hydrogen peroxide, or other chemicals, and oxidized cardiolipin has low affinity for NAO staining. Furthermore, in literature we can find several evidences demonstrating that cardiolipin oxidation is related to the apoptotic process (Kagan et al., 2005; Ott et al., 2007); then NAO staining not only provides a direct indication on structural integrity of the mitochondria but also indirectly suggests the activation of the intrinsic apoptotic pathway.

NAO MFIs (mean fluorescence intensities) evidence that all the chemicals used are able to trigger a mitochondrial impairment characterized by peroxidation (ROS induced) of cardiolipin (Fig. 7B)

Taking into account the MFI values for NAO labeling, an unusual pattern of peroxidation fluorescence at the single cell level can be identified after MEL administration in staurosporine treated samples, confirming electron microscopy observations.

Finally, to investigate whether MEL influenced injured myoblasts, western blotting was performed only for samples treated with etoposide and $H_2O_2$, as these agents are those that provide a more significant apoptotic effect. Our results revealed that these triggers induced a remarkable caspase-3 activation if compared to control and MEL treated cells. Moreover, MEL administration before chemical exposure down-regulated caspase-3 activation in both experimental conditions (Fig. 8), suggesting , a potential anti-apoptotic role for the pineal hormone.

**DISCUSSION**

This study aimed at the investigation of the effects of some of the most well-known chemicals known to induce apoptosis and at the study of MEL actions against these apoptotic triggers.

The obtained data indicate that a noteworthy apoptotic rate can be induced in myoblasts. All chemical treatments resulted in the alteration of cellular morphology with typical apoptotic features, such as membrane blebbing, chromatin condensation and micronuclei formation (even if the typical cup-shaped 'horse-shoe-like' chromatin patches were never observed) and finally production of apoptotic bodies. Autophagic features were also observed and, occasionally, secondary necrosis, particularly diffuse in staurosporine condition, appeared.

We observed that MEL *per se* is not harmful to cultured cells. Furthermore, it is able to significantly prevent the oxidative damage and/or cell death induced by various triggers, thanks to its powerful, direct and indirect, anti-oxidant action and to its known capacity to prevent mitochondrial dysfunctions (Hiboui et al., 2009; Wang et al., 2011; Teodoro et al., 2014; Yang et al., 2015). Data on cell viability, supported by ultrastructural analyses, demonstrated that MEL administration prevented cell death induced by chemical exposure, improving myoblast cyto/nuclear architecture stability, necessary for a correct fiber differentiation. Moreover, FC and quantitative results at fluorescence microscopy evidenced MEL ability to preserve mitochondrial membrane integrity, as well as to reduce ROS species accumulation.

In myoblasts, as expected, the most noticeable effect was found against $H_2O_2$. MEL action against etoposide appears weaker but significant, probably due to the multiple mechanisms of action of this chemical that involves, besides oxidative stress and the activation of the mitochondrial pathway, also damage at the nuclear level (Salucci et al, 2013; Salucci et al, 2014b; Sancho et al., 2014).

In the case of staurosporine treatment, only a weak protective effect was observed in samples treated for 5 hours and no protective effect was observed in those treated for 24 hours, suggesting only a delay in the apoptotic program. Staurosporine induces overlapping of distinct pathways of apoptosis, involving in part its ability to act as a non-selective inhibitor of a diverse array of different kinases and in part its ability to induce mitochondrial caspase activation (Stepczynska et al., 2001; Mele et al, 2014). However, the primary site of action of staurosporine in apoptosis induction is unknown and, given that MEL with its anti-oxidant action fails to hinder the activity of this drug, probably the main mechanism of staurosporine action does not pass through the ROS cascade.

Mitochondria are central executers of apoptosis by directly participating in caspase-dependent and caspase-independent cell death signaling (Dam et al., 2013) and here they seem to play a key role in highlighting MEL mechanism of action against apoptotic triggers in skeletal muscle cells.

It is known that impaired mitochondrial function, particularly related to those processes harbored in the inner mitochondrial membrane, might be associated to the disruption of the phospholipid environment (Bogdanov et al., 2008; Wang et al., 2011; Croston et al., 2013). Cardiolipin is a unique mitochondrial phospholipid, being primarily located in the inner mitochondrial membrane. Its content in mitochondria has been positively correlated to mitochondrial enzyme activities as NADH dehydrogenase, cytochrome *bc1* complex and cytochrome c oxidase (Bogdanov et al., 2008; Stefanyk et al., 2010). Growing evidences suggest that cardiolipin also controls mitochondrial biogenesis and cytochrome c release resulting in the activation of apoptosis (Houtkooper and Vaz, 2008; Paradies et al., 2009). Thus, even if undirectly, the measurement of its activity suggest the apoptotic involvement; in fact, cardiolipin evaluation at CLSM and after FC analyses evidences mitochondrial dysfunctions induced by chemicals that appeared restored in samples pre-treated with the neuro-hormone, in a significant way for $H_2O_2$ and etoposide, when cell death follows mitochondrial pathways and ROS cascades. In fact, analyses of both total cellular ROS and mitochondrial superoxide as well as cardiolipin peroxidation suggested that $H_2O_2$ and etoposide induce apoptosis primarily *via* the mitochondrial pathway. Thus MEL follows (although to a different extent) ROS-mediated mechanisms for exerting here the observed apoptotic protection: to maintain mitochondrial function, to reduce ROS level and to preserve mitochondrial membrane integrity. Moreover, MEL ability in preventing, at least in part, apoptotic cell death has been confirmed by the blotting results of caspase-3 activation after chemical exposure (etoposide and $H_2O_2$) showing its moderate reduction in myoblasts pre-treated with MEL before trigger administration, as also revealed by Stratos et al., 2012.

Taken together, these results suggest that MEL can protect skeletal myoblasts against mitochondrial-mediated apoptotic cell death acting, at least in part, through caspase-dependent mechanisms. Moreover, as evidenced by TB assay, MEL improves cell viability, potentially promoting mononucleated cell activation.

In conclusion, this study emphasizes MEL role as an effective anti-oxidant and anti-apoptotic molecule and confirms its hopeful application in protecting and regenerating muscle fibers in different muscular disorders

**References**

Abdel-Salam E, Abdel-meguid I, Korraa SS. 2009. Markers of degeneration and regeneration in Duchenne muscular dystrophy. *Acta Myol* 28: 94-100.

Avelar-Freitas BA, Almeida VG, Pinto MC, Mourão FA, Massensini AR, Martins-Filho OA, Rocha-Vieira E, Brito-Melo GE. 2014. Trypan blue exclusion assay by flow cytometry. *Braz J Med Biol Res* 47: 307-15.

Barbieri E, Agostini D, Polidori E, Potenza L, Guescini M, Lucertini F, Annibalini G, Stocchi L, De Santi M, Stocchi V. 2015. The pleiotropic effect of physical exercise on mitochondrial dynamics in aging skeletal muscle. Oxid Med Cell Longev 2015: 917085.

Battistelli M, Burattini S, Salucci S, Mariani AR, Falcieri E. 2011. Cell death induced by physical agents: morphological features. Microscopie doi: 10.4081/microscopie.2011.4976.

Battistelli M, Salucci S, Olivotto E, Facchini A, Minguzzi M, Guidotti S, Pagani S, Flamigni F, Borzì RM, Facchini A, Falcieri E. 2014. Cell death in human articular chondrocyte: a morpho-functional study in micromass model. Apoptosis 19: 1471-83.

Bennett BT, Mohamed JS, Alway SE. 2013. Effects of resveratrol on the recovery of muscle mass following disuse in the plantaris muscle of aged rats. PLoS One 8: e83518.

Bogdanov M, Mileykovskaya E, Dowhan W. 2008. Lipids in the assembly of membrane proteins and organization of protein supercomplexes: implications for lipid-linked disorders. Subcell Biochem 49: 197–239.

Burattini S, Salucci S, Baldassarri V, Accorsi A, Piatti E, Madrona A, Espartero JL, Candiracci M, Zappia G, Falcieri E. 2013. Anti-apoptotic activity of hydroxytyrosol and hydroxytyrosyl laurate. Food Chem Toxicol 55: 248-256.

Canonico B, Campana R, Luchetti F, Arcangeletti M, Betti M, Cesarini E, Ciacci C, Vittoria E, Galli L, Papa S, Baffone W. 2014. Campylobacter jejuni cell lysates differently target mitochondria and lysosomes on HeLa cells. Apoptosis 19: 1225-42.

Chahbouni M, Escames G, Venegas C, Sevilla B, García JA, López LC, Muñoz-Hoyos A, Molina-Carballo A, Acuña-Castroviejo D. 2010. Melatonin treatment normalizes plasma pro-inflammatory cytokines and nitrosative/oxidative stress in patients suffering from Duchenne muscular dystrophy. J Pineal Res 48: 282-289.

Chen Z, Chua CC, Gao J, Chua KW, Ho YS, Hamdy RC, Chua BH. 2009. Prevention of ischemia/reperfusion-induced cardiac apoptosis and injury by melatonin is independent of glutathione peroxdiase 1. J Pineal Res 46: 235-241.

Croston TL, Shepherd DL, Thapa D, Nichols CE, Lewis SE, Dabkowski ER, Jagannathan R, Baseler WA, Hollander JM. 2013. Evaluation of the cardiolipin biosynthetic pathway and its interactions in the diabetic heart. Life Sci 93: 313–322.

Dam AD, Mitchell AS, Quadrilatero J. 2013. Induction of mitochondrial biogenesis protects against caspase-dependent and caspase-independent apoptosis in L6 myoblasts. Biochim Biophys Acta 1833: 3426-35.

Davis J, Kwong JQ, Kitsis RN, Molkentin JD. 2013. Apoptosis repressor with a CARD domain (ARC) restrains Bax-mediated pathogenesis in dystrophic skeletal muscle. PLoS One 8: e8205.

Derbré F, Gratas-Delamarche A, Gómez-Cabrera MC, Viña J. 2014. Inactivity-induced oxidative stress: a central role in age-related sarcopenia?. Eur J Sport Sci 14: S98-108.

Ding K, Wang H, Xu J, Li T, Zhang L, Ding Y, Zhu L, He J, Zhou M. 2014. Melatonin stimulates antioxidant enzymes and reduces oxidative stress in experimental traumatic brain injury: the Nrf2-ARE signaling pathway as a potential mechanism. *Free Radic Biol Med* 73: 1-11.

Galano A, Tan DX, Reiter RJ. 2011. Melatonin as a natural ally against oxidative stress: a physicochemical examination. *J Pineal Res* 5: 1–16.

Guescini M, Guidolin D, Vallorani L, Casadei L, Gioacchini AM, Tibollo P, Battistelli M, Falcieri E, Battistin L, Agnati LF, Stocchi V. 2010. C2C12 myoblasts release micro-vesicles containing mtDNA and proteins involved in signal transduction. Exp Cell Res 316: 1977-84.

Han F, Tao RR, Zhang GS, Lu YM, Liu LL, Chen YX, Lou YJ, Fukunaga K, Hong ZH. 2011. Melatonin ameliorates ischemic-like injury-evoked nitrosative stress: Involvement of HtrA2/PED pathways in endothelial cells. J Pineal Res 50: 281–291.

Hardeland R, Tan DX, Reiter RJ. 2009. Kynuramines, metabolites of melatonin and other indoles: the resurrection of an almost forgotten class of biogenic amines. J Pineal Res 47: 109–126.

Hibaoui Y, Roulet E, Ruegg UT. 2009. Melatonin prevents oxidative stress-mediated mitochondrial permeability transition and death in skeletal muscle cells. J Pineal Res 47: 238-252.

Houtkooper RH, Vaz FM. 2008. Cardiolipin, the heart of mitochondrial metabolism. Cell Mol Life Sci 65: 2493–2506.

Jou MJ, Peng TI, Reiter RJ, Jou SB, Wu HY, Wen ST. 2004.Visualization of the antioxidative effects of melatonin at the mitochondrial level during oxidative stress-induced apoptosis of rat brain astrocytes. J Pineal Res 37: 55–70.

Kagan VE, Tyurin VA, Jiang J, Tyurina YY, Ritov VB, Amoscatom AA, Osipov AN, Belikova NA, Kapralov AA, Kini V, Vlasova II, Zhao Q, Zou M, Di P, Svistunenko DA, Kurnikov IV, Borisenko GG. 2005. Cytochrome c acts as a cardiolipin oxygenase required for release of proapoptotic factors. Nat Chem Biol 1: 223-232.

Korshunov SS, Skulachev VP, Starkov AA. 1997. High protonic potential actuates a mechanism of production of reactive oxygen species in mitochondria. FEBS Lett 416: 15-8.

Lee I, Bender E, Kadenbach B. 2002. Control of mitochondrial membrane potential and ROS formation by reversible phosphorylation of cytochrome c oxidase. Mol Cell Biochem 234-235: 63-70.

Loro E, Rinaldi F, Malena A, Masiero E, Novelli G, Angelini C, Romeo V, Sandri M, Botta A, Vergani L. 2010. Normal myogenesis and increased apoptosis in myotonic dystrophy type-1 muscle cells. Cell Death Differ 17: 1315-1324.

Marzetti E, Hwang JC, Lees HA, Wohlgemuth SE, Dupont-Versteegden EE, Carter CS, Bernabei R, Leeuwenburgh C. 2010. Mitochondrial death effectors: relevance to sarcopenia and disuse muscle atrophy. Biochim Biophys Acta 1800: 235-244.

Marzetti E, Csiszar A, Dutta D, Balagopal G, Calvani R, Leeuwenburgh C. 2013. Role of mitochondrial dysfunction and altered autophagy in cardiovascular aging and disease: from mechanisms to therapeutics. Am J Physiol Heart Circ Physiol 305: H459-76.

Mele A, Camerino GM, Calzolaro S, Cannone M, Conte D, Tricarico D. 2014. Dual response of the KATP channels to staurosporine: a novel role of SUR2B, SUR1 and Kir6.2 subunits in the regulation of the atrophy in different skeletal muscle phenotypes. Biochem Pharmacol 91: 266-75.
.

Merlini L, Angelin A, Tiepolo T, Braghetta P, Sabatelli P, Zamparelli A, Ferlini A, Maraldi NM, Bonaldo P, Bernardi P. 2008. Cyclosporin A corrects mitochondrial dysfunction and muscle apoptosis in patients with collagen VI myopathies. Proc Natl Acad Sci USA 105:5225-5229.

Ott M, Zhivotovsky B, Orrenius S. 2007. Role of cardiolipin in cytochrome c release from mitochondria. Cell Death Differ 14: 1243-1247.

Paradies G, Petrosillo G, Paradies V, Ruggiero FM. 2009. Role of cardiolipin peroxidation and Ca2 + in mitochondrial dysfunction and disease. Cell Calcium 45: 643–650.

Paradies G, Petrosillo G, Paradies V, Reiter RJ, Ruggiero FM. 2010. Melatonin, cardiolipin and mitochondrial bioenergetics in health and disease. J Pineal Res 48: 297–310.

Reiter RJ, Tan DX, Manchester LC, Pilar Terron M, Flores LJ, Koppisepi S. 2007. Medical implications of melatonin: receptor-mediated and receptor-independent actions. Adv Med Sci 52: 11-28.

Robinson KM, Janes MS, Pehar M, Monette JS, Ross MF, Hagen TM, Murphy MP, Beckman JS. 2006. Selective fluorescent imaging of superoxide in vivo using ethidium-based probes. Proc Natl Acad Sci U S A 103: 15038-43.

Salucci S, Battistelli M, Burattini S, Squillace C, Canonico B, Gobbi P, Papa S, Falcieri E. 2010a. C2C12 myoblast sensitivity to different apoptotic chemical triggers. Micron 41: 966-73.

Salucci S, Burattini S, Battistelli M, Chiarini F, Martelli AM, Sestili P, Valmori A, Gobbi P, Falcieri E. 2010b. Melatonin prevents hydrogen peroxide-induced apoptotic cell death. Microscopie doi: 10.4081/microscopie.2010.4970.

Salucci S, Burattini S, Baldassarri V, Battistelli M, Canonico B, Valmori A, Papa S, Falcieri E. 2013. The peculiar apoptotic behavior of skeletal muscle cells. Histol Histopathol 28: 1073-1087.

Salucci S, Burattini S, Curzi D, Buontempo F, Martelli AM, Zappia G, Falcieri E, Battistelli M. 2014a. Antioxidants in the prevention of UVB-induced keratynocyte apoptosis. J Photochem Photobiol B 142: 1-9.

Salucci S, Burattini S, Battistelli M, Baldassarri V, Curzi D, Valmori A, Falcieri E. 2014b. Melatonin prevents chemical-induced haemopoietic cell death. Int J Mol Sci 5: 6625-40.

Sancho M, Gortat A, Herrera AE, Andreu-Fernández V, Ferraro E, Cecconi F, Orzáez M, Pérez-Payá E. 2010. Altered mitochondria morphology and cell metabolism in Apaf1-deficient cells. PLoS One 9: e84666.

Shiokawa D, Kobayashi T, Tanuma S. 2002. Involvement of DNase gamma in apoptosis associated with myogenic differentiation of C2C12 cells. J Biochem Chem 277: 31031-31037.

Stefanyk LE, Coverdale N, Roy BD, Peters SJ, LeBlanc PJ. 2010. Skeletal muscle type comparison of subsarcolemmal mitochondrial membrane phospholipid fatty acid composition in rat. J Membr Biol 234: 207–215.

Stepczynska A, Lauber K, Engels IH, Janssen O, Kabelitz D, Wesselborg S, Schulze-Osthoff K. 2001. Staurosporine and conventional anticancer drugs induce overlapping, yet distinct pathways of apoptosis and caspase activation. Oncogene 20: 1193-1202.

Storz P. 2007. Mitochondrial ROS--radical detoxification, mediated by protein kinase D. Trends Cell Biol 17: 13-8.

Stratos I, Richter N, Rotter R, Li Z, Zechner D, Mittlmeier T, Vollmar B. 2012. Melatonin restores muscle regeneration and enhances muscle function after crush injury in rats. J Pineal Res 52: 62-70.

SullivanGunn MJ, Lewandowski PA. 2013. Elevated hydrogen peroxide and decreased catalase and glutathione peroxidase protection are associated with aging sarcopenia. BMC Geriatr 13: 104.

Teixeira vde O, Filippin LI, Xavier RM. 2012. Mechanisms of muscle wasting in sarcopenia. Rev Bras Reumatol 52: 252-259.

Teodoro BG, Baraldi FG, Sampaio IH, Bomfim LH, Queiroz AL, Passos MA, Carneiro EM, Alberici LC, Gomis R., Amaral FG, Cipolla-Neto J, Araújo MB, Lima T, Akira Uyemura S, Silveira LR, Vieira E. 2014. Melatonin prevents mitochondrial dysfunction and insulin resistance in rat skeletal muscle. J Pineal Res 57:155-167.

Vasilaki A, Jackson MJ. 2013. Role of reactive oxygen species in the defective regeneration seen in aging muscle. Free Radic Biol Med 65: 317-23.

Wang WZ, Fang XH, Stephenson LL, Zhang X, Khiabani KT, Zamboni WA. 2011. Melatonin attenuates I/R-induced mitochondrial dysfunction in skeletal muscle. J Surg Res 171: 108-13.

Yang Y, Jiang S, Dong Y, Fan C, Zhao L, Yang X, Li J, Di S, Yue L, Liang G, Reiter RJ, Qu Y. 2015. Melatonin prevents cell death and mitochondrial dysfunction via a SIRT1-dependent mechanism during ischemic-stroke in mice. J Pineal Res 58: 61-70.

Yoo YM, Jeung EB. 2009. Melatonin-induced estrogen receptor alpha-mediated calbindin-D9k expression plays a role in $H_2O_2$-mediated cell death in rat pituitary GH3 cells. J Pineal Res 47: 301–307.

Zhang HM, Zhang Y. 2014. Melatonin, a well-documented antioxidant with conditional pro-oxidant actions. J Pineal Res 57: 131–146.

**Figure Legends**

**Figure 1.** Histograms showing percentages of C2C12 cell viability/death obtained after TB analyses in all samples. In A, various MEL doses has been evaluated in C2C12 cells, evidencing that the lower ones induces a scarce death percentage. 100 or 50 µM mel have been evaluated against $H_2O_2$ demostrating that 100 µM is the concentration able to significantly prevent cell death (B). In C, cell viability analysis of control myoblasts, those exposed to chemical treatments and those pre-treated with MEL before chemicals. Student's t-Test shows that the decrease in cell death induced by MEL pre-treatment is highly statistically significant (**$p<0.01$) in $H_2O_2$ samples and it is statistically significant (*$p<0.05$) in etoposide . Data are from 3 independent experiments and are shown as mean±Standard deviation

.

**Figure 2.** Control C2C12 myoblasts (A, B, C, D) and myoblasts treated with 100 µM MEL (E, F, G, H). Cells were observed at SEM (A, E), at TEM (B, F) and at CLSM after TUNEL reaction (C, G) or NAO staining (D, H). A, C, E, F, H bar = 5µm; B bar = 2µm; D, G bar = 10µm.

**Figure 3**. C2C12 myoblasts exposed to $H_2O_2$ (A, B, C, D) and to MEL pre-treatment before $H_2O_2$administration(E, F, G, H). Cells were observed at SEM (A, F), at TEM (B, C, G) and at CLSM after TUNEL reaction (D, H) or NAO staining (E, I). A, D, F, G bar = 5µm; B bar = 2µm; C bar = 1µm; E, H, I bar = 10µm.

**Figure 4**. C2C12 myoblasts exposed to Etoposide (A, B, C, D) and to MEL pre-treatment before etoposide administration (E, F, G, H). Cells were observed at SEM (A, E), at TEM (B, F) and at CLSM after TUNEL reaction (C, G) or NAO staining (D, H). A, C, D, E, G, H bar = 5µm; B, F bar = 2µm.

**Figure 5.** C2C12 myoblasts exposed to staurosporine (A, B, C, D) and to MEL pre-treatment before staurosporine administration (E, F, G, H). Cells were observed at SEM (A, E), at TEM (B, F) and at CLSM after TUNEL reaction (C, G) or NAO staining (D, H). A, E bar = 5µm; B, F bar = 1µm; C, D, G, H bar = 10µm.

**Figure 6.** NAO mean fluorescence evaluation in C2C12 myoblasts (expressed in percentage) by means of Image J software . MEL prevents mitochondria membrane integrity in a significant way in the case of $H_2O_2$ (**$p<0.01$), etoposide (*$p<0.05$).

**Figure 7.** MitoSOX (A, grey) and CM-$H_2$CFDA (A, dark grey) analyses at FC on C2C12 myoblasts. Cellular distribution is given for MitoSOX and CM-H2CFDA fluorescence, comparing control myoblasts and $H_2O_2$-treated myoblasts (considered as representative treatment).
Statistic histogram related NAO (B) fluorescence detection shows that all triggers induce cardiolipin peroxidation and that melatonin is not able to prevent cardiolipin increase only in staurosporine–treated cells.
Data are from 3 separate experiments and are furnished as mean±SD

**Figure 8.** Caspase-3 activation, the cleaved one and Ponceau S red staining was reported as loading control analysis in C2C12 myoblasts (A). Caspase-3activation was quantified using the ratio cleaved caspase-3/caspase-3 (B).

FIGURE 1

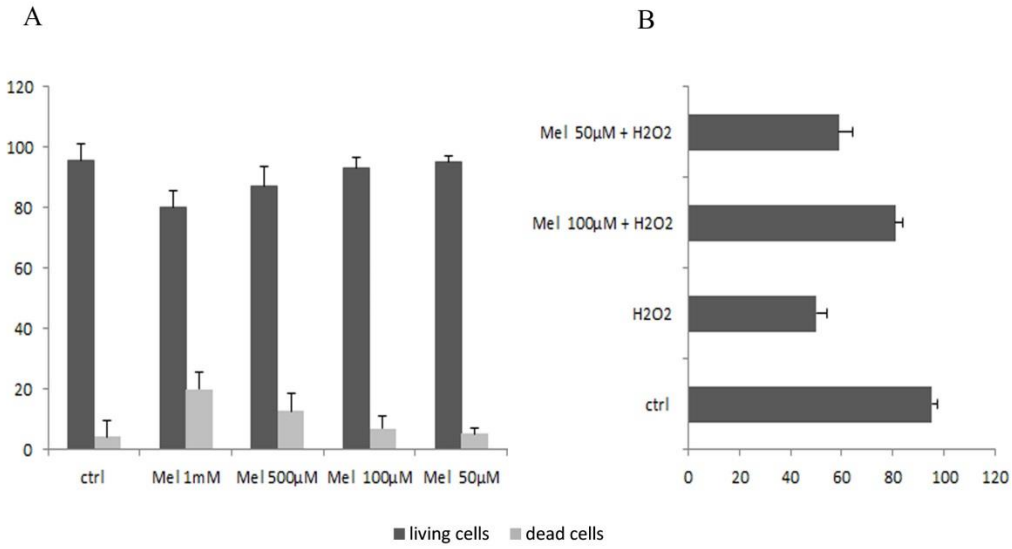
A
B
120
100
80
60
40
20
0
ctrl
Mel 1mM
Mel 500µM
Mel 100µM
Mel 50µM
Mel 50µM + H2O2
Mel 100µM + H2O2
H2O2
ctrl
0
20
40
60
80
100
120
living cells
dead cells

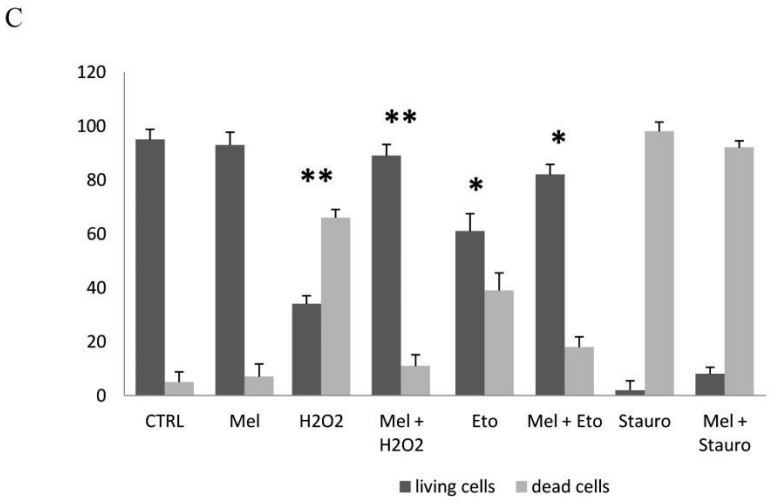
C
120
100
80
60
40
20
0
**
**
*
*
CTRL
Mel
H2O2
Mel + H2O2
Eto
Mel + Eto
Stauro
Mel + Stauro
living cells
dead cells

FIGURE 2

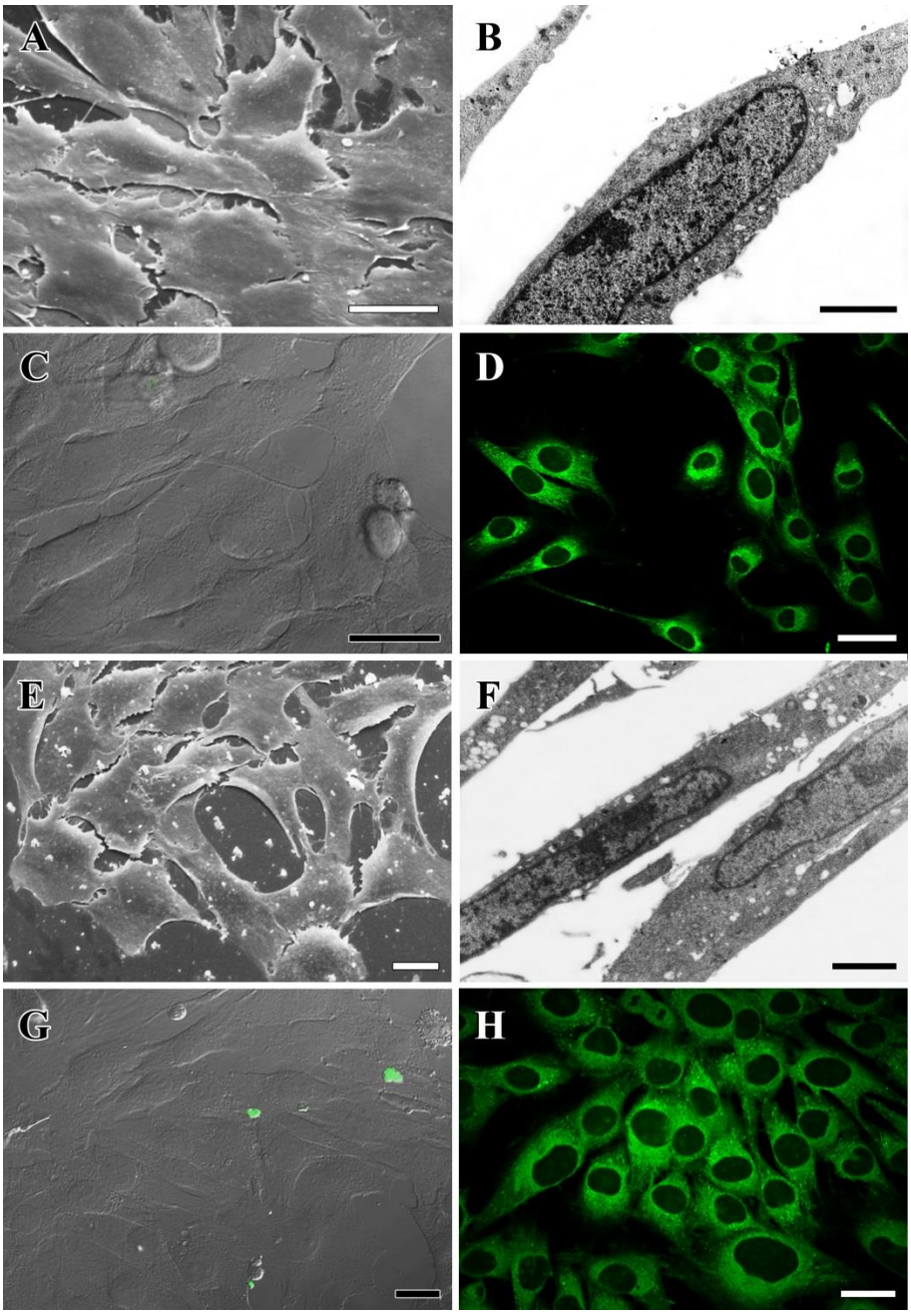

FIGURE 3

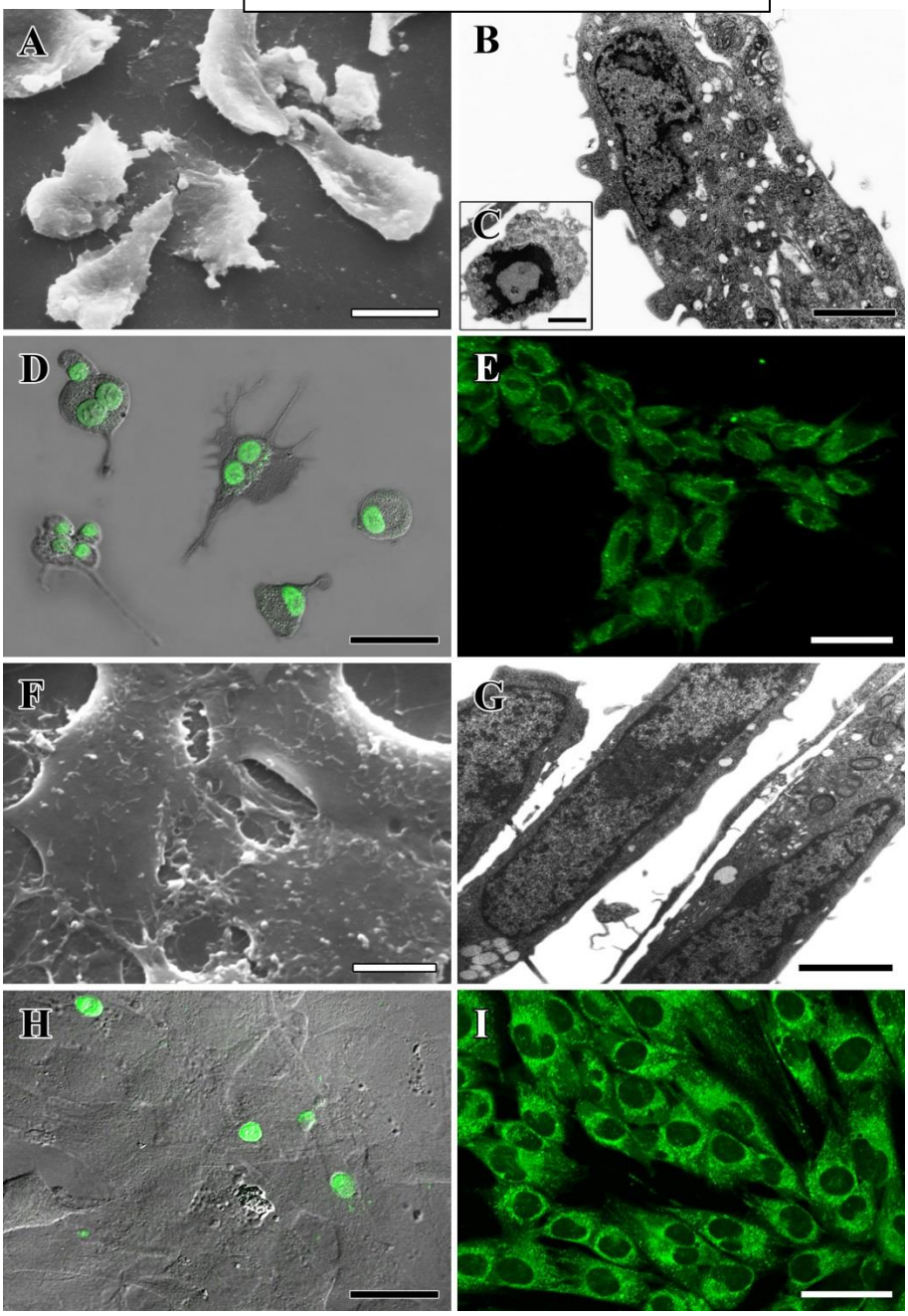

FIGURE 4

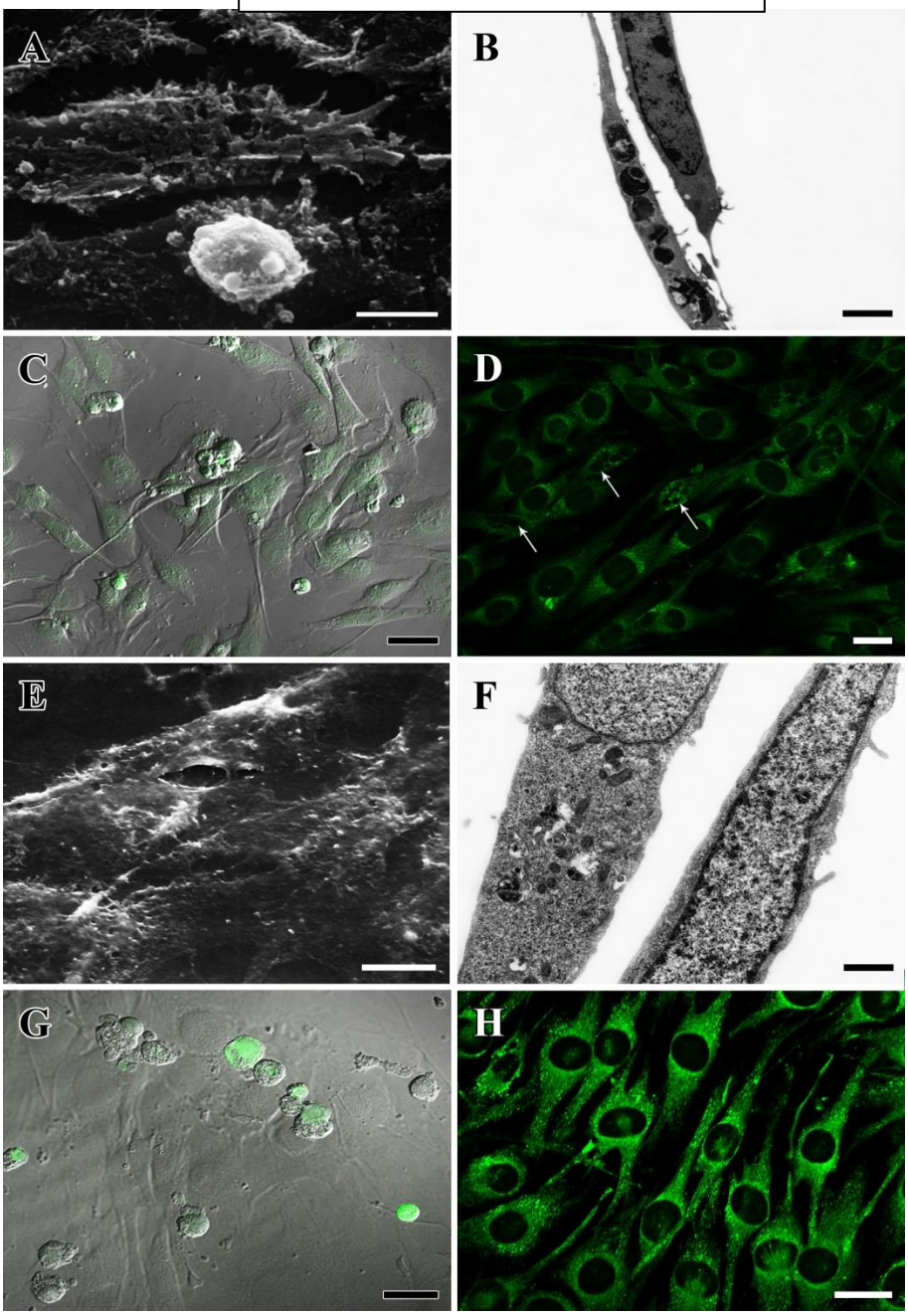

FIGURE 5

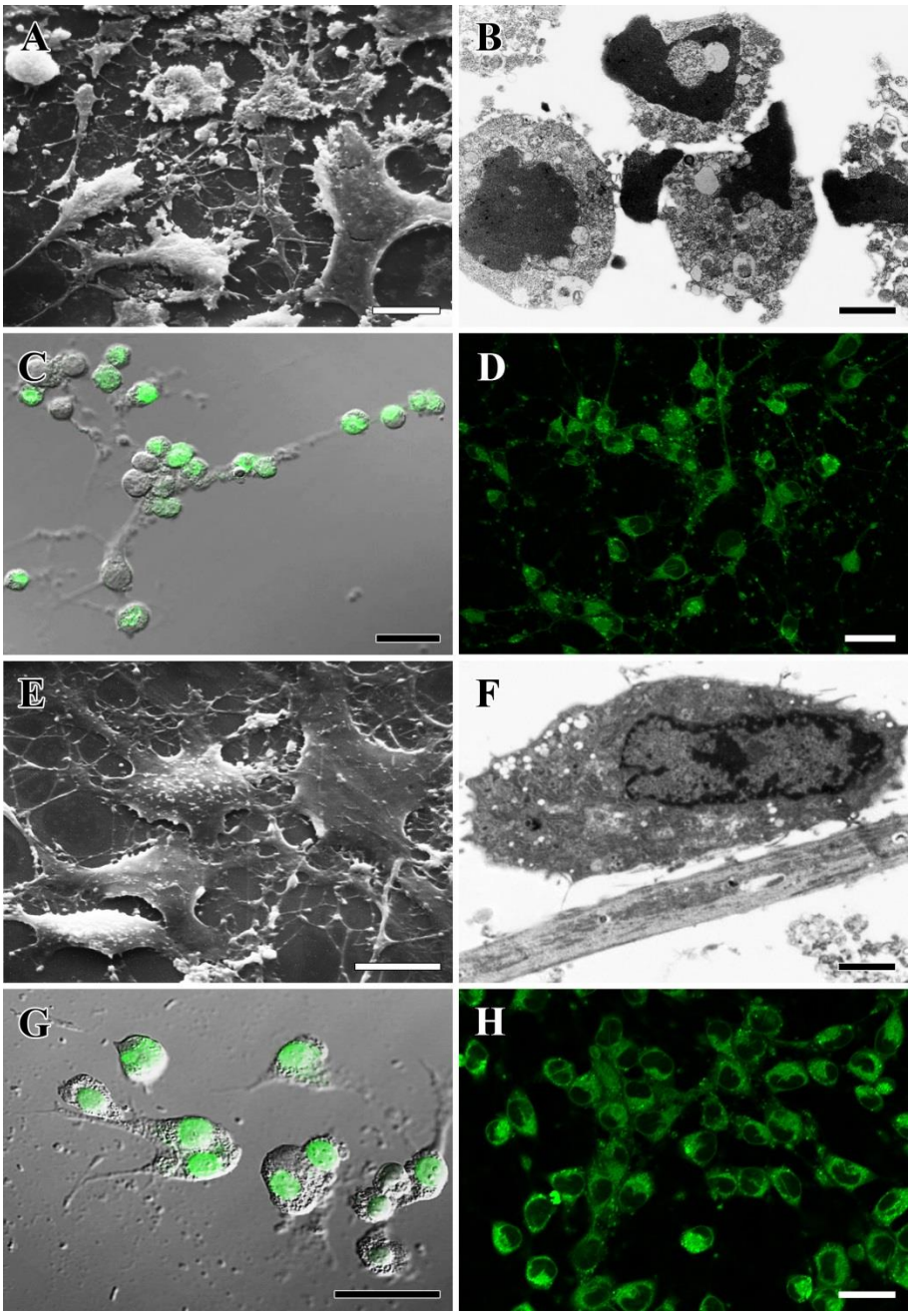

FIGURE 6

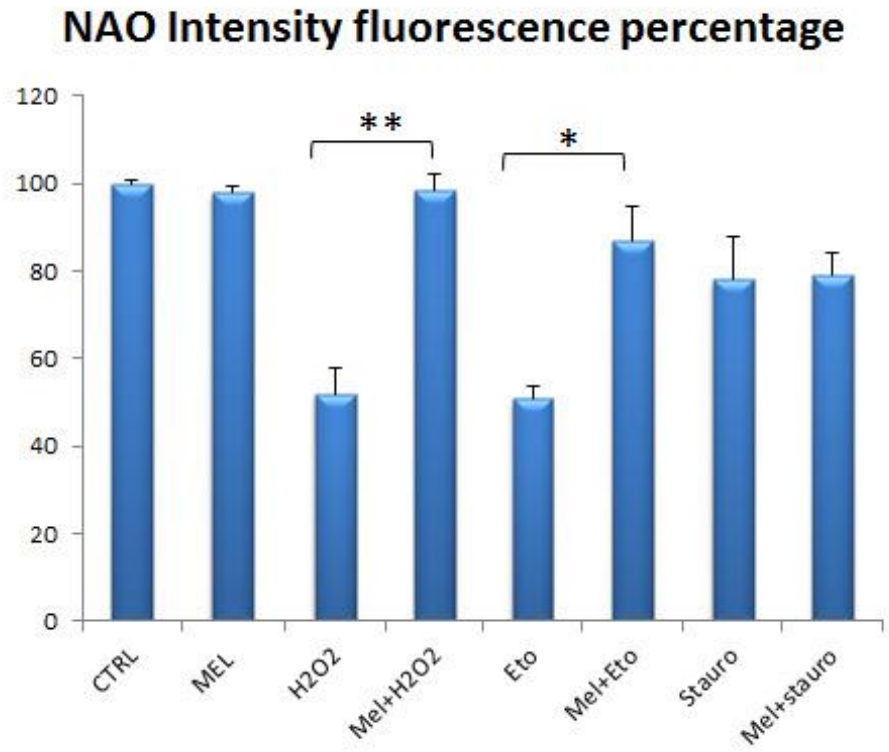
NAO Intensity fluorescence percentage
120
100
80
60
40
20
0
**
*
CTRL
MEL
H2O2
Mel+H2O2
Eto
Mel+Eto
Stauro
Mel+stauro

FIGURE 7

**A**

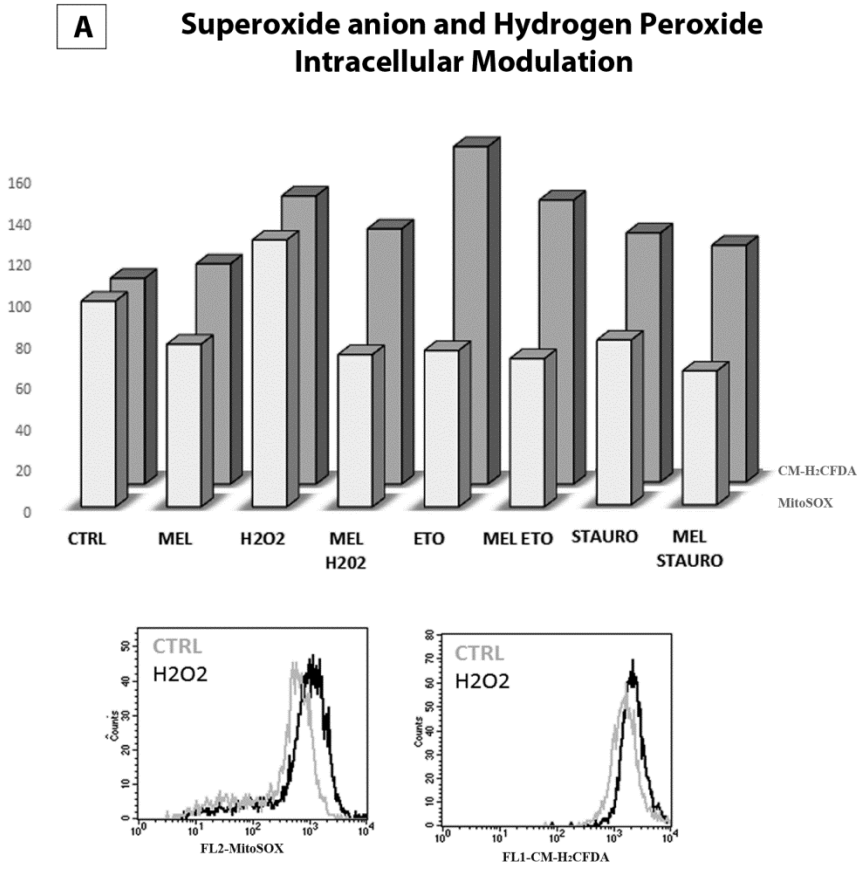
Superoxide anion and Hydrogen Peroxide Intracellular Modulation
160
140
120
100
80
60
40
20
0
CM-H2CFDA
MitoSOX
CTRL
MEL
H2O2
MEL H202
ETO
MEL ETO
STAURO
MEL STAURO
CTRL
H2O2
Counts
FL2-MitoSOX
CTRL
H2O2
Counts
FL1-CM-H2CFDA

**B**

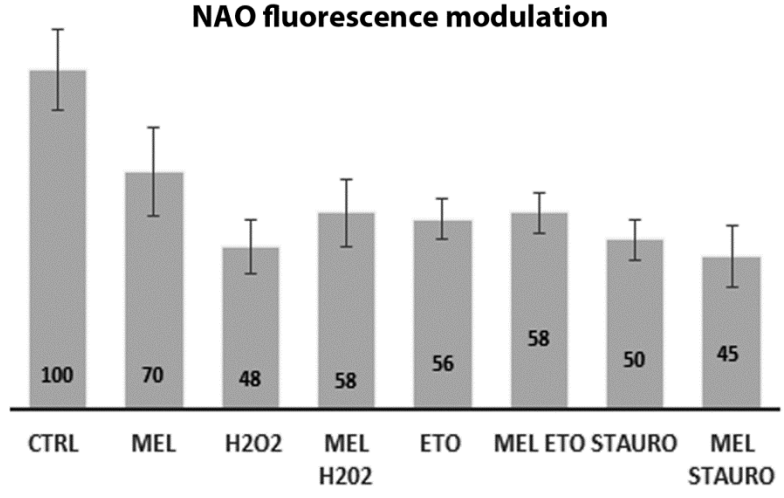
NAO fluorescence modulation
100
70
48
58
56
58
50
45
CTRL
MEL
H2O2
MEL H202
ETO
MEL ETO
STAURO
MEL STAURO

FIGURE 8

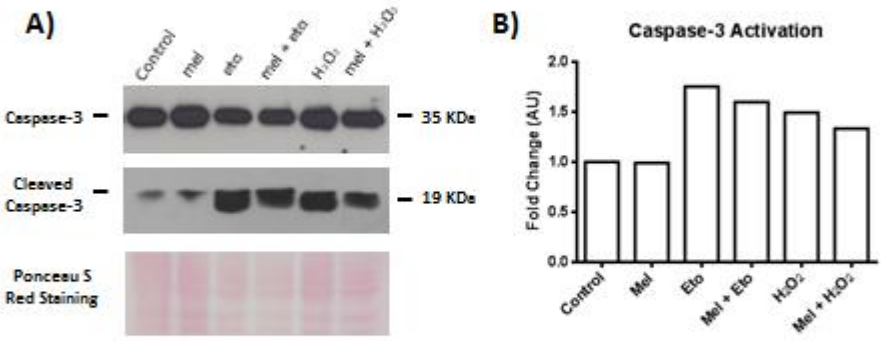
A)
Control
mel
eto
mel + eto
$H_2O_2$
mel + $H_2O_2$
Caspase-3
35 KDa
Cleaved Caspase-3
19 KDa
Ponceau S Red Staining
B)
Caspase-3 Activation
Fold Change (AU)
2.0
1.5
1.0
0.5
0.0
Control
Mel
Eto
Mel + Eto
$H_2O_2$
Mel + $H_2O_2$